

The hyperfine transition of $^3\text{He II}$ as a probe of the intergalactic medium

J.S. Bagla¹ and Abraham Loeb²

¹ Harish-Chandra Research Institute, Chhatnag Road, Jhusi, Allahabad 211019, India.

² Harvard-Smithsonian Center for Astrophysics, Mail Stop 51, 60 Garden Street, Cambridge, MA 02138, USA

E-Mail: ¹ jasjeet@hri.res.in, ² aloeb@cfa.harvard.edu

30 October 2018

ABSTRACT

We explore the prospects of using the hyperfine transition of $^3\text{He II}$ as a probe of the intergalactic medium. The emission signal from ionized regions during reionization is expected to be anti-correlated with 21 cm maps. The predicted emission signal from Ly- α blobs at lower redshifts is detectable with future radio observatories.

Key words: atomic processes, radiation mechanisms: general, cosmology : theory, early Universe, radio lines: general

1 INTRODUCTION

Galaxies form when gas in highly overdense haloes cools and collapses to form stars (Hoyle 1953; Rees & Ostriker 1977; Silk 1977; Binney 1977; White & Frenk 1991). The formation of the first stars (Bromm et al. 2009; McKee & Ostriker 2007; Zinnecker & Yorke 2007; Bromm & Larson 2004) led to emission of UV radiation that re-ionized the intergalactic medium (IGM) of hydrogen and helium (Loeb & Barkana 2001).

A number of methods can be used to probe the reionization process (Fan, Carilli, & Keating 2006), but the most promising probe appears to be the redshifted emission and absorption due to the hyperfine transition of neutral hydrogen with a rest frame frequency of 1.42 GHz (for a recent review see Furlanetto, Oh, & Briggs (2006)).

Singly ionized ^3He has a hyperfine transition similar to the 21 cm spin-flip transition of hydrogen. The astrophysical relevance of this transition was first pointed out by Townes (1957). Early studies focused on observing the transition from the interstellar medium, specifically from emission line nebulae (Sunyaev 1966; Goldwire & Goss 1967; Goldwire 1967). Several papers (Doroshkevich, Zel'Dovich, & Novikov 1967; Sunyaev & Zeldovich 1975; Furlanetto, Oh, & Briggs 2006) pointed out that this transition may potentially be used to probe early stages of galaxy formation.

Following the early theoretical work, attempts were made to observe this signal from nearby H II regions (Predmore et al. 1971), leading to the first detection by Rood et al. (1979). This line has been detected from a number of H II regions as well as a few planetary nebulae (Bell 2000; Balser et al. 2006, 2007). The primordial abundance of ^3He can be used to constrain big bang nucleosynthesis (Steigman 2007). The main challenge in observing this transition lies in separating it from recombination lines of hydrogen, which can be almost as strong if not stronger.

In this paper we explore the potential use of the hyperfine tran-

sition of $^3\text{He II}$ for studying the epoch of reionization (EoR) and the post-reionization IGM. In §2 we discuss aspects of the hyperfine transition for $^3\text{He II}$ and compare it with the corresponding transition of neutral hydrogen. Some sources and absorbers of this transition in the IGM are enumerated in §3. Finally, we consider in §4 the most promising sources from where $^3\text{He II}$ emission may be observed, and how future observations may constrain the EoR and the IGM. Throughout the paper, we adopt the WMAP-5yr values for the cosmological parameters (Komatsu et al. 2008).

2 HYPERFINE TRANSITION OF $^3\text{He II}$

We begin with a comparison of hyperfine transitions of H I and $^3\text{He II}$. For $^3\text{He II}$, the frequency of hyperfine transition is 8.66 GHz, much higher than 1.42 GHz frequency of the 21 cm transition of hydrogen. A higher frequency for the $^3\text{He II}$ hyperfine transition implies that the emission signal from the EoR is at frequencies where foregrounds are not as problematic as they are for 21 cm observations.

The magnetic moment of the ^3He nucleus is negative, and so the singlet is the excited state in the hyperfine transition while the triplet is the ground state. This is opposite of the situation in neutral hydrogen. As a result of the ground state being the triplet, emission is suppressed. The Einstein coefficient for the spontaneous decay of this transition is $A_{10} = 1.96 \times 10^{-12} \text{s}^{-1}$ (Sunyaev 1966; Goldwire & Goss 1967), which is ~ 700 times larger than the corresponding coefficient for the hyperfine transition of hydrogen. The effective gain is reduced by a factor of 3 due to the excited state being the singlet. The higher rate of emission implies a shorter lifetime for electrons in the excited state and this has interesting implications for observables, as shown in the discussion below.

The number density of ^3He atoms is a small fraction of the hydrogen density, the primordial ratio from big bang nucleosynthesis being close to 1.1×10^{-5} (Steigman 2007). The ionization

2 Bagla and Loeb

potential for hydrogen is 13.6eV, while the ionization potential for helium is 24.6eV for the first electron and 54.4eV for the second electron.

In analogy with the 21 cm transition, the optical depth for absorption of radiation from a background source by $^3\text{He II}$ is given by,

$$\begin{aligned} \tau_\nu &= \frac{1}{32\pi} \frac{hc^3 A_{10}}{k_B T_s \nu_0^2} \frac{x_{HeII} n_3 n_{He}}{(1+z)(dv_{\parallel}/dr_{\parallel})} \\ &= 6 \times 10^{-7} \frac{x_{HeII}}{T_s/\text{K}} (1+\delta)(1+z)^{3/2} \\ &\quad \times \left(\frac{n_3 n_{He}/n_H}{1.1 \times 10^{-5}} \right) \left[\frac{H(z)}{(1+z)(dv_{\parallel}/dr_{\parallel})} \right]. \end{aligned} \quad (1)$$

where $n_H \propto (1+z)^3$ is the primordial hydrogen density as a function of redshift z , $H(z) = H_0[\Omega_\Lambda + \Omega_m(1+z)^3]^{1/2}$ is the Hubble expansion rate (with Ω_Λ and Ω_m being the present-day density parameters of the cosmological constant and matter, $dv_{\parallel}/dr_{\parallel}$ is the comoving radial derivative of the radial velocity component of the cosmic gas along the line-of-sight (which equals $H(z)/(1+z)$ for the uniform background Universe), δ is the local overdensity of baryons, and x_{HeII} is the fraction of Helium atoms in the singly ionized state. The spin (excitation) temperature, T_s , is defined through the ratio between the number densities of hydrogen atoms in the excited and ground state levels,

$$\frac{n_1}{n_0} = \frac{g_1}{g_0} \exp\left\{-\frac{T_*}{T_s}\right\}, \quad (2)$$

where subscripts 1 and 0 correspond to the excited and ground state levels of the $^3\text{He II}$ transition, $T_* = h\nu/k_B = 0.42\text{K}$ is the temperature corresponding to the transition energy, and $(g_1/g_0) = 1/3$ is the ratio of the spin degeneracy factors of the levels.

The primary process that couples T_s with the gas temperature T_{gas} is the scattering of free electrons and $^3\text{He II}$ ions. There are two time scales of interest: the lifetime of an electron in the excited state, and the typical time between electron-ion collisions. Furthermore, we have to take into account the efficacy of collisions in setting the spin temperature. The ratio of the collision rate to the lifetime scales as $(1+z)^3(1+\delta)$. Thus, T_s and T_{gas} couple well at high redshifts or in regions with high overdensity. The Wouthuysen-Field effect (Field 1958, 1959; Wouthuysen 1952) is less relevant in coupling T_s with the gas temperature T_{gas} due to the proximity of the Ly- α lines for the two isotopes of Helium (Chuzhoy & Shapiro 2006). The color temperature is generally negative due to this proximity. In some situations in the interstellar medium, the proximity of the Ly- α lines for the two isotopes and an O III line can even lead to negative spin temperature (Deguchi & Watson 1985) in low density environments where collisions are not relevant and significant amount of He III is present.

For a fixed ionization fraction and a homogeneous Universe, the time evolution of the density of $^3\text{He II}$ ions in the ground state is given by,

$$\begin{aligned} \left(\partial_t + 3\frac{\dot{a}}{a}\right)n_0 &= -n_0(C_{01} + B_{01}I_\nu) \\ &\quad + n_1(C_{10} + A_{10} + B_{10}I_\nu), \end{aligned} \quad (3)$$

where $a(t) = (1+z)^{-1}$ is the cosmic scale factor, the A 's and B 's are the Einstein rate coefficients, the C 's are the collisional rate coefficients, and I_ν is the blackbody intensity in the Rayleigh-Jeans tail of the Cosmic Microwave Background (CMB), namely $I_\nu = 2k_B T_{\text{cmb}}/\lambda^2$ with the transition wavelength $\lambda = c/\nu = 3.46$ cm. The $0 \rightarrow 1$ transition rates can be related to the $1 \rightarrow 0$ transition rates by the requirement that in thermal equilibrium with

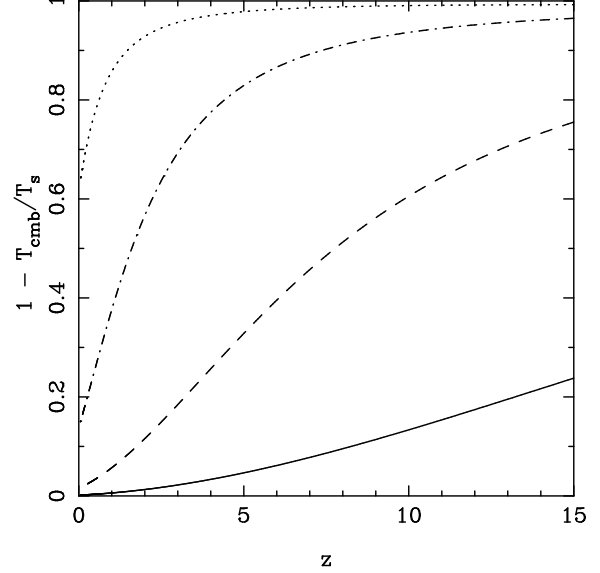


Figure 1. The coefficient $(1 - T_{\text{cmb}}/T_s)$ (to which the brightness temperature in Eq. (6) is proportional) as a function of redshift for regions of different values of overdensity, δ . The spin de-excitation rate is expressed as a fraction f_c of the value derived by Goldwire & Goss (1967). Different lines correspond to different values of $f_c(1+\delta)$, namely 1 (solid line), 10 (dashed line), 10^2 (dot-dashed line), and 10^3 (dotted line). We assume that hydrogen is fully ionized and helium is singly ionized, and that the gas temperature is 10^4 K.

$T_s = T_{\text{cmb}} = T_{\text{gas}}$ (where T_{gas} is the gas kinetic temperature), the right-hand-side of Eq. (3) should vanish with the collisional terms balancing each other separately from the radiative terms. This implies that $(C_{01}/C_{10}) = (g_1/g_0) \exp\{-T_*/T_{\text{gas}}\}$. We also use the standard relations $B_{10} = (\lambda^3/2hc)A_{10}$ and $B_{01} = (g_1/g_0)B_{10}$ (Rybicki & Lightman 1986). The collisional rates are proportional to the electron density n_e and depend on T_{gas} .

Equation (3) can be simplified to the form,

$$\begin{aligned} \frac{dY}{dz} &= -[H(1+z)]^{-1} [-Y(C_{01} + B_{01}I_\nu) \\ &\quad + (1-Y)(C_{10} + A_{10} + B_{10}I_\nu)], \end{aligned} \quad (4)$$

where $Y \equiv n_0/(n_0 + n_1)$. In the redshift range of interest, the Hubble expansion rate can be ignored relative to the atomic rate coefficients and so the left-hand-side of equation (4) can be approximately set to zero. For $T_s \gg T_*$ and $T_{\text{gas}} \gg T_*$, this yields the simple result (Furlanetto, Oh, & Briggs 2006; Pritchard & Loeb 2008),

$$T_s^{-1} = \frac{T_{\text{cmb}}^{-1} + x_c T_{\text{gas}}^{-1}}{1 + x_c}, \quad (5)$$

where $x_c = (T_*/T_{\text{cmb}})(C_{10}/A_{10})$.

The charged $^3\text{He II}$ ions interact with electrons through Coulomb collisions. The standard collision rate in a plasma receives equal contributions per logarithm of the impact parameter between the electron and the $^3\text{He II}$ ion, and so it includes the cumulative effect of many small-angle deflections of the electron (Spitzer 1998). However, most of the small angle scatterings will not result in a spin-flip transition for the bound electron. The maximum impact parameter of interest for exciting the $^3\text{He II}$ transition is set by the requirement that the energy transfer per single electron-ion col-

lision be larger than the $^3\text{He II}$ transition energy¹. For the distance of closest approach of a thermal electron relative to a $^3\text{He II}$ ion, the typical energy transfer is $\sim (m_e/m_{^3\text{He}})k_B T_{\text{gas}}$, amounting to ~ 1.7 K for $T_{\text{gas}} = 10^4$ K. The transition energy of 0.42K implies in this case a Coulomb logarithm of $\sim \ln(1.7/0.42) = 1.4$, which is an order of magnitude smaller than its maximum value, obtained from the cumulative effect of all scatterings with a smaller energy exchange². This implies that only a small subset (< 0.1) of all electron-ion collisions contribute. An estimate for the collisional coupling efficiency was derived by Goldwire & Goss (1967), based on the approach pioneered by Purcell & Field (1956); Field (1958, 1959). We quantify our collisional rate relative to this value.

Figure 1 shows the quantity $(1 - T_{\text{cmb}}/T_s)$ as a function of redshift for regions with different gas density contrast $(1 + \delta)$ relative to the cosmic mean. The results were derived assuming that hydrogen is fully ionized and helium is singly ionized, and that the gas temperature is 10^4 K. The spin de-excitation rate is proportional to the collisional rate, which in turn is proportional to $(1 + \delta)$. We take the spin de-excitation rate to be a fraction f_c of the Goldwire & Goss (1967) rate. Different lines correspond to different values of $f_c(1 + \delta)$, namely 1 (solid line), 10 (dashed line), 10^2 (dot-dashed line), and 10^3 (dotted line). The thick solid line that runs along the curve for $f_c(1 + \delta) = 1$ shows the collisional coupling estimate of Goldwire & Goss (1967). A more detailed calculation of the collisional rate can be made using spin-dependent scattering cross-sections (Jones et al. 1993; Hansen et al. 1995; Ishikawa et al. 1998).

Figure 1 indicates that the spin temperature of $^3\text{He II}$ decouples from the gas temperature at very high redshifts for regions at the average cosmic density. However, even for regions with an overdensity of ~ 10 , the spin temperature is only a few times the CMB temperature T_{cmb} through the EoR. This factor alone suppresses the signal from such regions by about 20% to 50%. Regions with much higher overdensity decouple only at late times and emission from such regions is not affected significantly at high redshifts. For example, at $z \simeq 3$ the low spin temperature leads to a reduction in the signal by about 20%. In general, the reduction in signal due to a low spin temperature is negligible for regions with electron number density $n_e \geq 10^{-2} \text{ cm}^{-3}$ if the Goldwire & Goss (1967) estimate is reliable.

During reionization, brightness fluctuations on large scales (tens of comoving Mpc or arc minutes on the sky) will be sourced by inhomogeneities in the $^3\text{He II}$ ionization fraction or in the kinetic temperature of the gas, which is heated to $\sim 10^4$ K in ionized regions (Trac, Cen, & Loeb 2008).

The absorption signal could be searched for in the radio spectrum of radio-loud quasars or gamma-ray burst afterglows (Ioka & Mészáros 2005). Absorption is expected to be weak in most situations, especially if the spin temperature is coupled to the kinetic temperature. The kinetic temperature in regions with substantial fraction of $^3\text{He II}$ is likely to be around 10^4 K and hence the optical depth due to absorption is extremely small in regions with $T_s \simeq T_{\text{gas}}$.

The brightness temperature for emission in the hyperfine transition of $^3\text{He II}$ is given by,

$$\delta T_b \simeq 18 \mu\text{K} x_{\text{HeII}} \left(1 - \frac{T_{\text{cmb}}}{T_s}\right) \left[\frac{1 + \delta}{10}\right] \left[\frac{1 + z}{9}\right]^{1/2}$$

¹ Following Field (1958), we ignore coupling of the incoming electron with the spin of the nucleus due to the larger mass of the nucleus.

² http://www.ppd.nrl.navy.mil/nrlformulary/NRL_FORMULARY_09.pdf

$$\times \left(\frac{n_{^3\text{He}}/n_{\text{H}}}{1.1 \times 10^{-5}}\right) \left[\frac{H(z)}{(1+z)(dv_{\parallel}/dr_{\parallel})}\right] \quad (6)$$

Since the first ionization of helium and hydrogen are expected to be contemporary (Wyithe & Loeb 2003), the power-spectrum of $^3\text{He II}$ brightness fluctuations during the hydrogen EoR can be calculated in analogy with the 21 cm power-spectrum (Pritchard & Loeb 2008). The $^3\text{He II}$ brightness temperature is smaller than that expected for the 21 cm transition of H I. However, the higher rest frame frequency compensates for the reduced signal, as the expected level of foregrounds increases sharply at lower frequencies. Thus, observing this signal is not as difficult as might seem at a first glance. Of course, for a system to be seen in emission it must have $T_s > T_{\text{cmb}}$. Figure 1 may serve as a guide in gauging the significance of the term $(1 - T_{\text{cmb}}/T_s)$. We discuss specific sources in the following section.

3 DISCUSSION

Next we discuss prospects of observing systems the hyperfine transition of $^3\text{He II}$ in emission during and after the EoR. The expected signal is weak, and there is a further attenuation due to decoupling of gas temperature and spin temperature in regions that are not very overdense. Thus, the most promising sources that may be detected and studied are those that are sufficiently overdense.

Ly- α blobs, first discovered by Steidel et al. (2000), are of particular interest. By now, many such blobs have been detected (Steidel et al. 2000; Nilsson et al. 2006; Yang et al. 2009), including one at a redshift $z = 6.6$ (Ouchi et al. 2009). These blobs are hundreds of kpc across and contain gas at a high overdensity. The leading theoretical model for these blobs is accretion of cold gas at temperatures around 10^4 K along filaments (Dijkstra & Loeb 2009). Irrespective of the detailed model, we can trivially deduce that gas in these blobs is at temperatures around 10^4 K as much hotter gas will not emit much in Ly- α , and that the overdensities in these blobs are fairly high, certainly of the order of 10^2 if not more. This makes such blobs a very strong source of radiation in the hyperfine transition of $^3\text{He II}$. If we assume that $\delta \sim 10^2 - 10^3$ (a reasonable assumption since we are dealing with gas inside collapsed haloes), $x_{\text{HeII}} \sim 0.5$, and $[dv_{\parallel}/dr_{\parallel}]/[H(z)/(1+z)] \sim 0.1 - 1$, the estimated $^3\text{He II}$ signal is in the range of 10–500 μK . Since a large number of Ly- α blobs are known, a targeted study is possible. Observations of blobs in the hyperfine transition of $^3\text{He II}$ can provide a direct handle on the physical properties of the sources. The number density of Ly- α blobs is sufficiently high (Dijkstra & Loeb 2009) so that blind searches can also be undertaken in the redshifted radiation from the hyperfine transition of $^3\text{He II}$.

H II regions around clusters of the earliest galaxies are also an obvious source of this radiation. For typical stellar sources, ^3He is expected to be ionized together with hydrogen since its first ionization potential is only a factor of 1.8 times larger (Wyithe & Loeb 2003). Observational constraints on reionization models suggest that normal stars may suffice as a source of ionizing radiation and enrichment of the IGM (Daigne et al. 2006; Bagla, Kulkarni, & Padmanabhan 2009). We therefore expect that tracing $^3\text{He II}$ at redshifts $z > 7$ is equivalent to tracing the H II regions. A map of $^3\text{He II}$ of a representative cosmic volume during reionization would therefore largely appear as the contrast of a 21 cm map of the same volume. Anti-correlating the two signals would be helpful in strengthening the signal-to-noise ratio of both maps. In addition, a measurement of the $^3\text{He II}$ signal can

be used (in conjunction with 21 cm data) to determine the cosmic ${}^3\text{He}$ abundance as a test of big bang nucleosynthesis. Note that for sources at redshift $z \simeq 15$, the observed frequency is close to 550 MHz and is in the regime where the sky temperature is subdominant to the system temperature for most existing and planned instruments. At high redshifts, even regions with moderate overdensities can be seen in emission.

In case of sources with a harder spectrum, we expect an inner region dominated by He III. The recombination time for He III is much smaller as compared to He II. This leads to formation of fossil ${}^3\text{He}$ II regions if the source of hard radiation switches off for an extended period of time. Quasars are the most obvious source of hard UV radiation and these are known to have intermittent periods of activity. Therefore fossil ${}^3\text{He}$ II regions at high redshift are also a promising source of signal.

Several existing and upcoming instruments have the required frequency coverage to attempt observations of the hyperfine transition in ${}^3\text{He}$ II. We summarize some of these here:

- The Giant Meterwave Radio Telescope (GMRT)³ located near Pune, India, has been in operation for over a decade and its performance is being enhanced through upgrades. The complete frequency range 1 – 1.42 GHz is available, allowing observations of the hyperfine transition of ${}^3\text{He}$ II between $5.1 \leq z \leq 7.6$, at least in principle. The best sensitivity achieved so far is $30 \mu\text{Jy}^4$. This is close to two orders of magnitudes larger than the sensitivity required to observe Ly- α blobs, hence it will be difficult to use the GMRT for observing Ly- α blobs at high redshifts even with long integrations on a single source, unless upcoming upgrades can reduce the noise level by a significant amount.

- The Expanded Very Large Array (EVLA)⁵, is an upgraded version of the very large array (VLA). This facility will enter a testing phase with science projects in 2010 and is likely to be available for all users by 2013. EVLA will have full coverage from 1 GHz to 50 GHz and hence can be used to probe ${}^3\text{He}$ II redshifts up to $z = 7.6$. The low frequency system is to be installed last. The overall sensitivity is slightly less than that for ASKAP.

- The Australian Square Kilometer Array Pathfinder (ASKAP)⁶ will comprise an array of 36 antennas each 12 m in diameter, capable of high dynamic range imaging and using wide-field-of-view phased array feeds. This observatory is expected to become operational by 2013. Frequencies between 700 MHz and 1.8 GHz will be accessible using ASKAP indicating that it may be possible to observe up to $z \sim 11.4$. The stated sensitivity will be insufficient for observing Ly- α blobs with around 10^3 hours of integration time. However, the field of view for this instrument is large and it may be possible to run a piggyback survey where co-adding the signal from many known Ly- α blobs may be used to enhance the signal-to-noise ratio.

- The Square Kilometer Array (SKA)⁷ is expected to have an effective collecting area that is nearly two orders of magnitudes larger than SKA pathfinders like the ASKAP. This alone ensures that observations of Ly- α blobs will be possible with the SKA with an integration of just above a hundred hours.

Finally we comment on the issue of foregrounds. The sky temperature T_{sky} is a very strong function of frequency at low fre-

quencies, scaling as $\nu^{-2.7}$ at low frequencies ($\lesssim 1$ GHz). Given the difference in rest frame frequencies of the hyperfine transition of neutral hydrogen and ${}^3\text{He}$ II, the expected difference in the sky temperature for observing the same redshift differs by a factor of almost 200. This nearly compensates for the difference in the expected signals for the two transitions at the highest redshifts of interest for the epoch of reionization studies. At lower redshifts, $T_{\text{sys}} > T_{\text{sky}}$ for most upcoming arrays and the instrumental noise is the dominant factor. Furthermore, the higher frequency implies that the Sun and ionosphere are not very serious problems and day time observations may also be possible, thereby increasing the possible integration time on one source.

For redshifts beyond 5.1, H I at low redshifts is a foreground contaminant for the hyperfine transition of ${}^3\text{He}$ II. This is not likely to be a cause for concern for targeted studies but is an issue for statistical detection. One may either choose *clean* lines of sight, or use differences in the angular and redshift space distribution of foregrounds as compared to the signal.

Recombination lines of hydrogen can be a source of confusion, particularly if the number densities of electrons are more than a few per cm^{-3} . Observations of H II regions (Balsler et al. 2006) find several lines of this type near the ${}^3\text{He}$ II hyperfine transition. The impact of such lines on cosmological observations has been found to be small by Oh & Mack (2003).

4 SUMMARY

In this paper we have considered the use of the hyperfine transition of ${}^3\text{He}$ II for studies of the IGM, with an emphasis on the possibility of detecting it in emission. The frequency of the ${}^3\text{He}$ II transition is ~ 6 times larger while its radiative decay rate is almost three orders of magnitude higher than those of the 21 cm transition of hydrogen. These parameters lead to a weaker coupling between the kinetic temperature of the IGM and the ${}^3\text{He}$ II spin temperature. However, ${}^3\text{He}$ II naturally exists in regions where the gas temperature is relatively high ($\sim 10^4$ K) and even this weak coupling can ensure $T_s \gg T_{\text{cmb}}$ in moderately overdense regions.

Although the abundance of ${}^3\text{He}$ is around 10^{-5} times that of hydrogen, its hyperfine signal is boosted by its higher decay rate. Additional gain in the signal-to-noise ratio originates from the lower sky temperature at the frequency of the ${}^3\text{He}$ II transition as compared with the sky temperature for the 21 cm radiation at the same redshift. Thus, observing the ${}^3\text{He}$ II signal may not be much more challenging than observing the redshifted 21 cm signal.

The higher rest frame frequency of the hyperfine transition of ${}^3\text{He}$ II also allows one to probe physical scales that are six times smaller, as compared to those that can be accessed with the 21 cm radiation using the same instrument for a region at the same redshift.

We find that the extended Ly- α blobs seen at high redshifts are the most promising source in this transition and that ${}^3\text{He}$ II observations may shed new light on the physical conditions in these regions. A number of Ly- α blobs are already known and it is possible to conduct a targeted study. The expected signal of $10\text{--}200 \mu\text{K}$ should be within the reach of upcoming instruments. In the longer term, observations of the hyperfine transition in ${}^3\text{He}$ II may be used to probe cosmological H II regions during the EoR.

³ <http://gmrt.ncra.tifr.res.in>

⁴ See page 9 of http://www.ncra.tifr.res.in/~gtac/GMRT_specs_status_Dec08.pdf

⁵ <http://www.aoc.nrao.edu/evla/>

⁶ <http://www.atnf.csiro.au/projects/askap/>

⁷ <http://www.skatelescope.org/>

ACKNOWLEDGMENTS

This work was supported in part by Harvard University funds and NASA grant NNX08AL43G. This research has made use of NASA’s Astrophysics Data System. We acknowledge the use of the Legacy Archive for Microwave Background Data Analysis (LAMBDA). Support for LAMBDA is provided by the NASA Office of Space Science.

While this project was nearing completion, we learned of a similar effort on $^3\text{He II}$ hyperfine emission by M. McQuinn, & E. R. Switzer (2009, submitted to Phys. Rev. D). We refer the reader there for complementary discussion.

REFERENCES

Bagla J. S., Kulkarni G., Padmanabhan T., 2009, MNRAS in Press, (arXiv:0902.0853)

Balser, D. S., Goss, W. M., Bania, T. M., & Rood, R. T. 2006, ApJ, 640, 360

Balser, D. S., Rood, R. T., & Bania, T. M. 2007, Science, 317, 1171

Bell, M. B. 2000, ApJ, 531, 820

Binney J., 1977, ApJ, 215, 483

Bromm V., Larson R. B., 2004, ARA&A, 42, 79

Bromm V., Yoshida N., Hernquist L., McKee C. F., 2009, Nature, 459, 49 (arXiv:0905.0929)

Chuzhoy L., Shapiro P. R., 2006, ApJ, 651, 1

Cox, A. N. (ed) 2000, Allen’s Astrophysical Quantities, 4th ed. Publisher: New York: AIP Press; Springer.

Daigne F., Olive K. A., Silk J., Stoehr F., Vangioni E., 2006, ApJ, 647, 773

Deguchi, S., & Watson, W. D. 1985, ApJ, 290, 578

Dijkstra M., Loeb A., 2009, arXiv:0902.2999

Doroshkevich A. G., Zel’Dovich Y. B., Novikov I. D., 1967, SvA, 11, 233

Fan X., Carilli C. L., Keating B., 2006, ARA&A, 44, 415

Field G. B., 1959, ApJ, 129, 536

Field G. B., 1958, Proc. I.R.E., 46, 240

Furlanetto S. R., Oh S. P., Briggs F. H., 2006, PhR, 433, 181

Goldwire H. C., 1967, PhRvL, 18, 433

Goldwire H. C., Jr., Goss W. M., 1967, ApJ, 149, 15

Hansen J.-O., et al., 1995, PhRvL, 74, 654

Hoyle F., 1953, ApJ, 118, 513

Ishikawa S., Golak J., Witała H., Kamada H., Glöckle W., Hüber D., 1998, PhRvC, 57, 39

Jones C. E., et al., 1993, PhRvC, 47, 110

Komatsu E., et al., 2009, ApJS, 180, 330 (arXiv:0803.0547)

Loeb A., Barkana R., 2001, ARA&A, 39, 19

McKee C. F., Ostriker E. C., 2007, ARA&A, 45, 565

Ioka, K., & Mészáros, P. 2005, ApJ, 619, 684

Nilsson K. K., Fynbo J. P. U., Møller P., Sommer-Larsen J., Ledoux C., 2006, A&A, 452, L23

Oh, S. P., & Mack, K. J. 2003, MNRAS, 346, 871

Ouchi M., et al., 2009, ApJ, 696, 1164

Predmore, C. R., Goldwire, H. C., Jr., & Walters, G. K. 1971, ApJ Letters, 168, L125

Pritchard J. R., Loeb A., 2008, PhRvD, 78, 103511

Purcell E. M., Field G. B., 1956, ApJ, 124, 542

Rees M. J., Ostriker J. P., 1977, MNRAS, 179, 541

Rood, R. T., Wilson, T. L., & Steigman, G. 1979, ApJ Letters, 227, L97

Rybicki G. B., Lightman A. P., 1986, *Radiative Processes in Astrophysics*, Wiley-VCH

Silk J., 1977, ApJ, 211, 638

Spitzer L., 1998, *Physical Processes in the Interstellar Medium*, Wiley-VCH

Steidel C. C., Adelberger K. L., Shapley A. E., Pettini M., Dickinson M., Giavalisco M., 2000, ApJ, 532, 170

Steigman G., 2007, ARNPS, 57, 463

Sunyaev R. A., 1966, AZh, 43, 1237

Sunyaev R. A., Zeldovich I. B., 1975, MNRAS, 171, 375

Townes C. H., 1957, IAUS, 4, 92

Trac H., Cen R., Loeb A., 2008, ApJ, 689, L81

White S. D. M., Frenk C. S., 1991, ApJ, 379, 52

Wouthuysen S., 1952, Phy, 18, 75

Wyithe J. S. B., Loeb A., 2003, ApJ, 586, 693

Yang Y., Zabludoff A., Tremonti C., Eisenstein D., Davé R., 2009, ApJ, 693, 1579

Zinnecker H., Yorke H. W., 2007, ARA&A, 45, 481